International Journal of Technology 13(5) 1149-1158 (2022)
Received April 2022 / Revised August 2022 / Accepted August 2022

International Journal of Technology

http://ijtech.eng.ui.ac.id

Modelling Human-Structure Interaction in Sideways Fall for Hip Impact Force Estimation

Lin Wei Lau[1], Chee Kuang Kok[2*], Gooi Mee Chen[2], Chih-Ping Tso[2]

[1]*Pixel Automation Pte Ltd, 10 Admiralty Street #04-13 North Link Building Singapore, Singapore 757695*
[2]*Center for Advanced Mechanical and Green Technology, Faculty of Engineering and Technology, Multimedia University, Jalan Ayer Keroh Lama, 75450 Bukit Beruang, Melaka, Malaysia*

Abstract. Sideways fall-induced hip fracture is a primary global health concern among the elderly. Existing impact models for predicting peak hip impact force mostly consider the human body-related parameters rather than impact surface parameters. This study proposed improving existing spring-mass-damper models by accounting for the human-structure dynamic interaction during sideways fall for better predicting peak impact force on the hip. Information required to construct the models was extracted from the literature. Different peak hip impact forces were estimated by considering differences in gender, body height, body mass, stiffness, damping coefficients of body tissue over the greater trochanter, and the impact surface stiffness. The predicted peak hip impact forces were compared to measured or simulated results in the literature and found to agree reasonably. Simulation results show that interactions with impact surfaces with lower stiffness can reduce the value of peak impact force applied on the hip by at least 16%.

Keywords: Flooring material; Hip fracture; Impact force attenuation; Spring-mass-damper; Trochanteric tissue stiffness

1. Introduction

Sideway fall often results in osteoporotic hip fracture, which is a major health care issue over the world that leads to immobility or even death (Nor-Izmin et al., 2020). According to statistics (Burns & Kakara, 2018), 55% of unintentional injuries among Americans over the age of 65 were caused by falls. Major clinical risk assessment tools available today including bone densitometry based on hip Dual-energy X-ray absorptiometry (DXA), hip structural analysis (HSA), and fracture risk assessment tool (FRAX) (Sarvi & Luo, 2015) could provide hip fracture risk assessment due to sideways fall with reasonable accuracy (Sarvi & Luo, 2017). None of them accounts for the stiffness and damping of the trochanteric tissue, and a person's body anthropometric parameters directly related to the fallen body effective mass, which significantly affect the hip impact force (Sarvi & Luo, 2017; Choi, 2013).

Biomechanics models (Kroonenberg et al., 1995) have shown that effective mass can vary from 25% to 75% of the overall mass depending on different kinematic configurations right before the fall impact. Sarvi and Luo (2015) proposed a framework for estimating hip fracture risk that has become widely accepted. This framework uses anthropometric data

*Corresponding author's email: ckkok@mmu.edu.my, Tel.: +60-6-2523648; Fax: +60-6-2316552
doi: 10.14716/ijtech.v13i5.5824

from DXA images to construct a dynamic model to predict the impact force. Subsequently, proximal femur DXA data is used to construct a finite element (FE) model to estimate the contact forces or stresses that are induced around the femoral head by the impact force. FE models have been widely used in biomechanics to simulate knee or hip arthroplasty (Ahmad et al., 2020; Triwardono et al., 2021). Fleps et al. (2019) developed FE models to predict the impact forces on human cadaveric hips and femoral heads embedded in ballistic gelatine with reasonable accuracy. Recently, Khakpour et al. (2021) studied the effect of impact velocity, flooring material, and trochanteric tissue by developing FE models and observed that bone quality and trochanter thickness had a more significant influence over the flooring type and trochanter stiffness on hip fracture. Kok et al. (2021) performed ex vivo full-field strain measurements on femoral necks under sideways fall conditions using digital image correlation to validate their FE models. They found that the experimental peak force correlated strongly with the predicted fracture force. Fung et al. (2022) used FE models to evaluate the efficacy of prophylactic femoral augmentation systems to reduce the risk of hip fracture during sideways falls. Abe et al. (2022) built 111 proximal femur FE models to simulate hip fracture risk in athletes, and non-athletes in different directions of sideways falls. However, due to research ethics, those findings cannot be verified using data from living humans. In addition, such FE models required detailed modeling of tissue and bone geometry, as well as local bone stiffness, besides making assumptions of trochanteric tissue and hip cartilage behavior. A computationally less intensive model that does not require specialists knowledge will be more desirable. Such attempts were made by Zijden et al. (2017) and Sarvi and Luo (2019). To estimate the peak hip impact force, the former created a generic multi-linear regression model that accounted for different subject-specific and kinematic variables. However, the trained model was empirical and lacked a physical basis. The latter developed a female-specific equation to predict the peak hip impact force without considering the effect of flooring materials.

Previous research (Sarvi & Luo, 2017; Groen, et al., 2008) concluded that many external factors influence the hip impact force during a fall, some of which are subject-specific and/or circumstantial and difficult to predict before a fall. Among them are 1) the arrest mechanisms employed by a falling person, 2) his initial fall conditions and fall configuration, which affects his hip vertical velocity immediately before impact, and 3) the human body interactions with the floor (Shaabpoor & Pavic, 2016). The peak hip impact force could have been overestimated by 38% in the presence of interactions between lightweight flooring and the fallen body (Shaabpoor & Pavic, 2016). It was reported that soft flooring such as tatami could reduce peak impact force by more than 60% (Li et al., 2013). No physical non-finite element model approximates the force attenuation caused by soft flooring. Hence, this study aims to develop a non-subject-specific model that accounts for the human-floor interaction during a sideways fall in estimating hip peak impact force. The model will consider important factors such as the fallen person's gender, body weight, height, and dynamic interactions with the impact surface. The authors will illustrate how, in most cases, the body mass index (BMI) and gender alone, rather than age and trochanteric tissue thickness, are sufficient intermediate predictors of a person's effective stiffness and damping ratio, leading to impact force predictions.

2. Methods

2.1. Model Development

Sarvi and Luo's framework (2015) was adopted in developing our peak hip force model. The authors' model is made up of two sub-models that work sequentially. First, a dynamic sub-model determines the effective mass and the impact velocity of the fallen

body. Second, an impact sub-model predicts the peak hip force based on two spring-mass-damper stacked in series. For the dynamic sub-model, a two-link model with a 45-degree inclined torso (a.k.a. jack-knife) (Kroonenberg et al., 1995) was used for simulating sideways fall from a standing position, and a point mass dynamic model for simulating very short-distance sideways hip release experiment (Laing et al., 2006). Therefore, the impact velocity, v (m/s), and effective mass, m_{eff} (kg), reduce to:

$$v = 2.72\sqrt{h} \text{ (for jack-knife)} \quad (1a)$$

$$v = \sqrt{2gH} \text{ (for point mass)} \quad (1b)$$

$$m_{eff} = 0.35m \text{ (for jack-knife)} \quad (2a)$$

$$m_{eff} = 0.43m \text{ (for point-mass)} \quad (2b)$$

where h is the height (in unit m) of the falling person, and H is the effective mass drop height. The selection of the two-link model was based on the fact that this model exhibited the lowest error (i.e., 22% to 36%) among the non-subject specific models (Sarvi & Luo, 2017). This error stems from the inability to predict the non-deterministic fall configurations of individuals.

The stiffness and damping coefficients of the trochanteric tissue are key parameters in the impact sub-model. Recent findings on these coefficients will be presented first, followed by the justification of the current model. There are contradicting views on how age and soft tissue thickness (STT) affect trochanteric tissue stiffness and damping coefficients. Sarvi and Luo (2017) remarked that stiffness and damping coefficients of trochanteric tissue are related to STT, apart from gender, age, BMI, and body configurations during impact. Choi (2013) and Choi et al. (2015) found that there was little statistical correlation between STT and tissue stiffness among young and older women, and that aging reduced tissue stiffness in older women. Lim and Choi (2019) state that the trochanter soft tissue stiffens with age. Moreover, a standardized method for measuring trochanter soft tissue stiffness and damping coefficients has yet to be agreed upon. The stiffness obtained by curve-fitting impact force data on the hip (Robinovitch et al., 1991; Sarvi et al., 2014; Nasiri & Luo, 2016) can be significantly larger than that measured from an indenter device (Choi, 2013; Robinovitch et al., 1995; Laing & Robinovitch, 2008). For example, stiffness and damping coefficient of 72.7 kN/m < k < 108.4 kN/m and 641 Ns/m < c < 860 Ns/m in Ref. (Sarvi, et al., 2014) are almost 2-3 times those reported in Ref. (Choi, 2013) and (Robinovitch et al., 1995). In view of the contradictions in previous work, it may be sufficient to represent parameters such as tissue thickness, gender, BMI, and age by just tissue effective stiffness and damping coefficients.

It is also very likely that the stiffness of the tissue is nonlinear (Choi et al., 2015; Laing & Robinovitch, 2010; Makhsous et al., 2008). For an individual with average weight, it could be induced from Makhsous et al.'s (2008) data that the stiffness became 2.24-fold when the trochanter soft tissue thickness was 18.65% compressed. And since the soft tissue has a definite thickness, it defies physics to allow compression beyond its own thickness. This work assumes that tissue stiffness will further increase by 0.5-fold at 37.3% (i.e., 2 X 18.65%) compression and beyond. In addition, gelatine simulating human tissue is twice as stiff as actual human tissue based on Farrer et al.'s work (2015).

To model the effect of the impact surface, two spring-mass-dampers are stacked to form a two-degree-of-freedom vibration system, as illustrated in Figure 1. In this figure, M is the mass, K is the spring stiffness, and C is the damping coefficient. The subscripts h and f represent the falling human and the impacted floor, respectively.

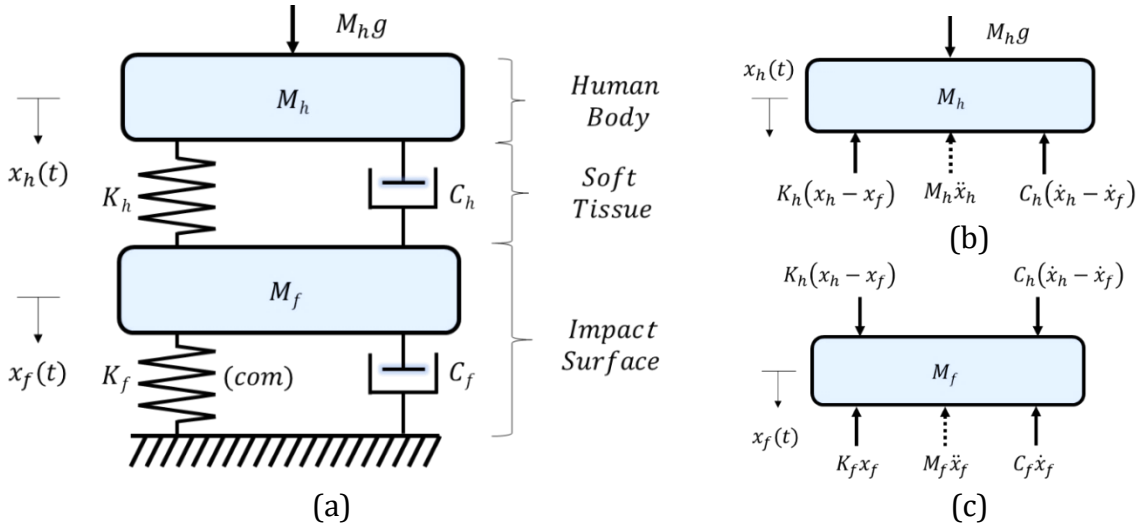

Figure 1 (a) Two-degree of freedom impact model; (b) Free body diagram of the falling person, with hip tissue stiffness and damping; (c) Free body diagram of the floor, with impact surface stiffness and damping.

This model is very similar to Shahabpoor and Pavic's (2016) model, with the following key differences: 1) no agent-based modeling was used to couple the two mass-spring-damper systems. Hence the current model can only be used to predict the peak impact force and not the force undulations afterward; 2) tissue stiffness is modeled as a trilinear spring instead of a bilinear spring in this work and 3) the stiffness and coefficients of the model in this work is extracted from experimental measurements by other researchers (Nasiri & Luo, 2016), and not pre-determined before simulation.

2.2. Numerical Implementation

The impact sub-model was implemental via the Newmark method (Chopra, 2017). The governing differential equations of the impact model can be written in a 2×2 matrix as shown in Equation (3).

$$\begin{bmatrix} M_h & 0 \\ 0 & M_f \end{bmatrix}\begin{bmatrix} \ddot{x}_h \\ \ddot{x}_f \end{bmatrix} + \begin{bmatrix} C_h & -C_h \\ -C_h & C_f + C_h \end{bmatrix}\begin{bmatrix} \dot{x}_h \\ \dot{x}_f \end{bmatrix} + \begin{bmatrix} K_h & -K_h \\ -K_h & K_f + K_h \end{bmatrix}\begin{bmatrix} x_h \\ x_f \end{bmatrix} = \begin{bmatrix} M_h g \\ 0 \end{bmatrix} \quad (3)$$

In Newmark numerical implementation, a time-stepping method is applied to variables at increments. The constant average acceleration Newmark Beta method (Chopra, 2017) is adopted to compute the displacement (x_i), velocity ($\dot{x}_i$), and acceleration ($\ddot{x}_i$) of the human mass and the floor surface, respectively. The method is unconditionally stable and can be summarized in Equations (4) and (5):

$$\dot{x}_{i+1} = \dot{x}_i + 0.5[\ddot{x}_i + \ddot{x}_{i+1}](\Delta t) \quad (4)$$

$$x_{i+1} = x_i + \dot{x}_t(\Delta t) + 0.25[\ddot{x}_i + \ddot{x}_{i+1}](\Delta t)^2 \quad (5)$$

The generalized external forces, P, in *i+1* increment, are described in Equations (6) and (7): -

$$P_{h,i+1} = M_h g + C_h \dot{x}_{f,i} + K_{h,i} x_{f,i} \quad (6)$$

$$P_{h,i+1} = M_h g + C_h \dot{x}_{f,i} + K_{h,i} x_{f,i} \quad (7)$$

Here, the first subscript of the variables denotes the object (i.e., human or floor), and the second subscript after the comma indicates the increment. The solutions for the equations of motion are as follows:

$$x_{i+1} = \frac{\hat{p}_{i+1}}{\hat{k}} \tag{8}$$

$$\dot{x}_{i+1} = \frac{2}{\Delta t}(x_{i+1} - x_i) - \dot{x}_i \tag{9}$$

$$\ddot{x}_{i+1} = \frac{4}{\Delta t^2}(x_{i+1} - x_i) - \frac{4}{\Delta t}\dot{x}_i - \ddot{x}_i \tag{10}$$

where

$$\hat{k} = K + \alpha_1 \tag{11a}$$

$$\hat{p}_{i+1} = P_{i+1} + \alpha_1 x_i + \alpha_2 \dot{x}_i + \alpha_3 \ddot{x}_i \tag{11b}$$

$$\alpha_1 = \frac{4}{\Delta t^2} M + \frac{2}{\Delta t} C \tag{11c}$$

$$\alpha_2 = \frac{4}{\Delta t} M + C \tag{11d}$$

$$\alpha_3 = M \tag{11e}$$

The variables M, K, C, and P in Equations (8) to (10) are to be substituted with corresponding mass, spring stiffness, damping coefficients, and residual force of the human or the floor, according to Equations (6) and (7), respectively. $\hat{k}$ and $\hat{p}$ are the effective stiffness and effective load factor, respectively. The solution is obtained first on the human and then on the impact floor and repeated until the specified end time.

The initial stiffness (K_1) damping coefficients and estimated thickness of human tissues (STT) over the greater trochanter used in this study were as reported in (Nasiri & Luo, 2016). Table 1 shows the mean stiffness data reduced to simple regressions with correlation coefficients greater than 0.94. Damping coefficients were treated as categorical data corresponding to BMI and gender categories (Nasiri & Luo, 2016). Furthermore, the trochanteric tissue stiffness was represented by a trilinear nested-spring design in Fig 2, and K_1 is the tissue stiffness according to Equations (12b) and (13b). It should be noted that the stiffness and damping coefficients of the greater trochanter tissue reported in (Nasiri & Luo, 2016) were originally obtained by Robinovitch et al. (1991) who curve-fit the experimental force responses of male and female participants in pelvis-release experiments into an impact model. Therefore, these values to the extent allowable in the experiments, accounted for the mechanics of muscles, tendons, and fat making up the greater trochanter (Kani et al., 2016) under sideways fall compression.

Table 1 Simple regressions between BMI, STT, and mean stiffness

Gender	Variable	Expression	
Male	STT (mm)	STT = 3.8429*BMI - 45.254	(12a)
	K (kN/m)	K = 395.6*(BMI)$^{-0.755}$	(12b)
Female	STT (mm)	STT = 2.4991*BMI - 14.189	(13a)
	K (kN/m)	K = 1935.6*(BMI)$^{-1.4}$	(13b)

The effective stiffness and effective damping coefficient of an impact surface used in the current study were taken from Ref. (Laing et al., 2006). Table 2 depicts the range of effective stiffness of compliant flooring as reported by Laing et al. (2006), on a mat of 1.85 x 0.6 m with varying thickness. The mass of the impact surface was computed from the mat

area in contact with the hip, estimated at 0.04 m^2 benchmarking the head of the impactor in Ref. (Li et al., 2013), along with the reported density of 46.6 kg/m^3 and thickness in Table 2 for the ethylene vinyl acetate foam. The damping ratio of the flooring material is assumed to be 0.1. For rigid flooring, the mass and stiffness values can be set to extremely high values.

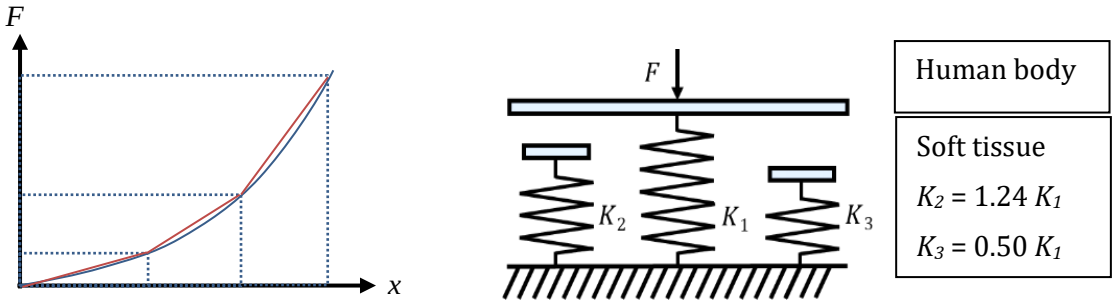

(a) (b)

Figure 2 (a) Trilinear approximation (i.e., three red lines to approximate the blue curve); (b) Nested spring representation of trilinear tissue stiffness.

Table 2 Effective stiffness of compliant flooring (Laing et al., 2006)

Floor Type	Floor Thickness (cm)	Flooring Stiffness, k (kN/m)
Rigid	NIL	~∞
Firm	1.5	263
Semifirm	4.5	95
Semisoft	7.5	67
Soft	10.5	59

3. Results and Discussion

3.1. Fall on Rigid Flooring

The predictions of impact forces using the proposed model will be verified using four different cases of sideways fall or small-distance hip release on rigid flooring from the literature. The input parameters and predicted impact force are summarized in Table 3. Case 1 is a simulated sideways fall from standing height on a rigid impact surface on non-subject-specific individuals. Case 2, a protected fall experiment by Sarvi et. al (2014), simulates fall from standing height but with initial kinematic configurations using a sling and harness on subject-specific individuals. Case 3 has to do with a very short-distance (i.e. 5 cm) sideways hip release experiment on 15 young women to study the effect of compliant flooring to impact force attenuation (Laing, et al., 2006). Finally, Case 4 mimics elderly standing-height sideways falls using gelatine-embedded cadaveric pelvic constructs (Fleps, et al., 2019).

In estimating peak impact force due to a sideways fall from standing height in Case 1, the interaction between a human body with a rigid flooring was simulated. The mean values of human body parameters (as in Table 4) were taken from the Centers for Disease Control and Prevention (Radzevičienė & Ostrauskas, 2013). The model predicted peak impact forces to be 4777 N and 3245 N, for males and females, respectively. This averages out to be 4011 N for both genders, which is close to the reported peak impact force in the range of 4050 to 6420 N (Sarvi & Luo, 2017). It, however, under-predicted the mean hip peak force of 5200 N reported by Sarvi and Luo (2017) by 22.9% but is within the already known margin of errors of the jack-knife model. The simulations are presented in a plot of force as a function of time in Fig. 3. It is good to note in passing that the aim of the model is to predict

the peak impact force. Therefore, the undulation of the force due to rebound after the first peak can be ignored.

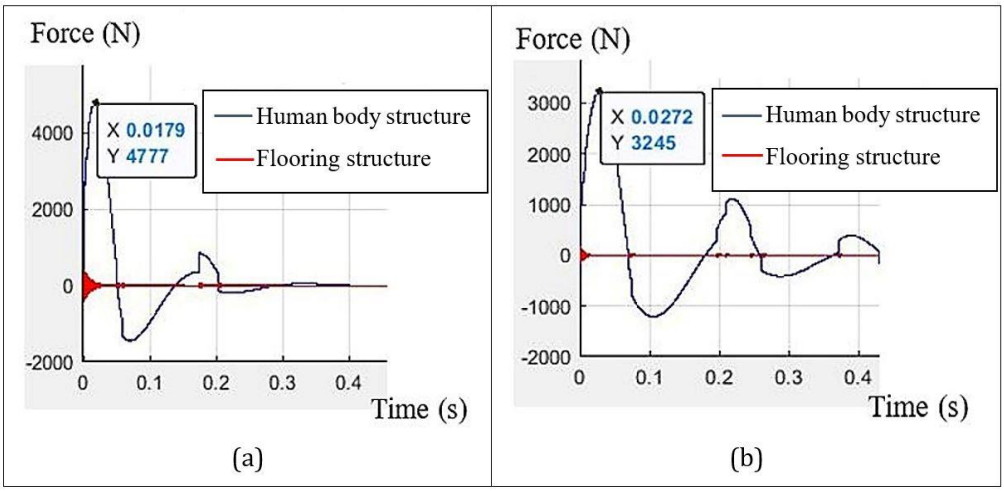

Figure 3 Predicted peak impact force for (a) male and (b) female with mean heights and mass

Table 3 Input parameters and predicted impact force for four different cases on rigid flooring

		Input				Output: Hip Peak Impact force (N)		
Case/ Input	Gender	Height (m)	Weight (kg)	Impact Velocity (m/s)	Effective Mass (kg)	Experiment	Model	Percent Error
Case 1	Male	1.757	88.8	Eq (1a)	Eq (2a)	From 4050 to 6420	4777	Within Range
	Female	1.616	76.4	Eq (1a)	Eq (2a)		3245	19.9%
Case 2 (Sarvi, et al., 2014)	Male	1.73	77	1.063	35.56	1900.8	1722	9.4%
	Male	1.72	72	1.236	29.75	1714.4	1905	11.1%
	Male	1.74	64	2.493	24.62	2961.8	3406	15.0%
Case 3 (Laing, et al., 2006)	Female	1.70	59.6	Eq (1b)	Eq (2b)	1059±42	1273	16%
Case 4 (Fleps, et al., 2019)	Female	1.63	40.8	3.1	Eq (2b)	2910	5145	76.8%
	Female	1.78	49.0	3.1	Eq (2b)	6131	5627	8.2%
	Female	1.65	59.0	3.1	Eq (2b)	5641	4797	15.0%
	Female	1.68	61.3	3.1	Eq (2b)	4907	4869	0.8%
	Female	1.63	84.0	3.1	Eq (2b)	4958	4305	13.2%
	Female	1.58	99.8	3.1	Eq (2b)	4910	3950	19.6%
	Male	1.75	45.4	3.1	Eq (2a)	5242	5840	11.4%
	Male	1.83	63.5	3.1	Eq (2a)	5043	6193	22.8%
	Male	1.75	68.1	3.1	Eq (2a)	7601	6105	19.7%

Using the current impact model in Case 2, experimental peak hip impact forces and the predictions agree with experiments to within 15% of error, although the drop configurations and subsequent kinematics were subject-specific in the experiment. Unlike the work of Laing and Robinovitch (2010) and Laing et al. (2006), the predictions made in this study in Case 3 did not require actual measurements of effective mass or velocity. The model and experiment results agree to within 16% error.

Similarly, when benchmarked against Fleps et al. (2019) experimental results in Case 4, the predictions made in this study did not employ full-scale finite element models with accurate bone geometry and bone material properties. It is worth noting that the current

model has overestimated the peak hip impact force for the first female scenario but agreed with the experimental measurement by having at most 23% error in all the other scenarios.

3.2. Fall on Non-rigid Flooring

Laing et al. (2006) measured the peak hip impact forces on females (mean weight of 59.6 kg and height of 170 cm) using 5-cm pelvis drop experiments and two different postures on flooring materials listed in Table 2 to simulate sideways falls. 6%-19% attenuation was observed in the experimental peak hip impact forces on the different compliant flooring relative to rigid flooring. The results of this comparison are summarized in Table 4.

Table 4 Hip impact force attenuation

Floor Type	% attenuation (Laing, et al., 2006)	% attenuation (Current study)
Firm	6-10	16
Semi-firm	14-16	23
Semisoft	15-18	25
Soft	16-19	27

Although the current model slightly overpredicted the percent attenuation in the simulated fall experiments by an extra 6-8%, the trend of decreasing gain in the attenuation rate from semi-firm to soft flooring material matches the observation in Ref. (Laing et al., 2006) well. The 6-8% extra attenuation could be taken as the percent error of the model, and the error may have come from the uncertainty related to the prediction of trochanteric tissue stiffness based on BMI and gender.

4. Conclusions

The authors demonstrated that factors such as body height, body weight (and thence BMI), gender of the individuals, and impact velocity alone appear sufficient in a non-subject-specific model for estimating the peak hip impact force. In contrast, age and actual trochanteric tissue thickness may be less significant. Except for one scenario, the proposed model could predict the mean peak hip impact force of a sideways fall from standing height with 77% accuracy. The amount of attenuation indicated in the hip impact force (i.e., 16%-27%) due to compliant flooring also agrees with previous work (i.e., 6%-19%). Regressions were made on the trochanteric tissue stiffness in published literature. The predictions were made using a tri-linear spring-mass-damper stacked model, and no individual measurements of trochanteric tissue stiffness and damping coefficients were required. To be sure, the inclusion of a third spring in the trilinear spring model is not entirely justified. More testing may be required to validate its use.

Acknowledgements

This research work has not received any grant from any funding agency. The authors are grateful to Multimedia University for granting them access to a MATLAB license to produce this work.

References

Abe, S., Kouhia, R., Nikander, R., Narra, N., Hyttinen, J., Sievanen, H., 2022. Effect of Fall Direction on the Lower Hip Fracture Risk in Athletes with Different Loading Histories: A Finite Element Modeling Study in Multiple Sideways Fall Configurations. *Bone*, Volume 158, p. 116351

Ahmad, M.A., Zulkifli, N.N.M.E., Shuib, S., Sulaiman, S.H., Abdullah, A.H., 2020. Finite Element Analysis of Proximal Cement Fixation in Total Hip Arthroplasty. *International Journal of Technology*, Volume 11(5), pp. 1046–1055

Burns, E., Kakara. R., 2018. Deaths from Falls Among Persons Aged ≥65 Years — the United States, 2007–2016. *MMWR. Morbidity and Mortality Weekly Report*, Volume 67(18), pp. 509–514

Choi, W., Russell, C., Tsai, C., Arzanpour, S., Robinovitch, S., 2015. Age-related Changes in Dynamic Compressive Properties of Trochanteric Soft Tissues Over the Hip. *Journal of Biomechanics*, Volume 48(4), pp. 695–700

Choi, W.J., 2013. *Biomechanics of Falls and Hip Fractures in Older Adults*. Master's Dissertation, Graduate Program, Simon Fraser University, Burnaby, British Colombia, Canada

Chopra, A.K. 2017. Dynamics of Structures: Theory and Applications to Earthquake Engineering. *Hoboken*, NJ: Pearson

Farrer, A.I., Odeen, H., Christensen, D.A., 2015. Characterization and Evaluation of Tissue-mimicking Gelatin Phantoms for Use with MRgFUS. *Journal of Therapeutic Ultrasound* Volume 3(9), pp. 1–11

Fleps, I., Guy, P., Ferguson, S.J., Cripton, P.A., Helgason, B., 2019. Explicit Finite Element Models Accurately Predict Subject-Specific and Velocity-Dependent Kinetics of Sideways Fall Impact. *Journal of Bone and Mineral Research,* Volume 34(10), pp. 1837–1850

Fung, A., Fleps, I., Cripton, P.A., Guy, P., Ferguson, S.J., Helgason. B., 2022. Prophylactic Augmentation Implants in the Proximal Femur for Hip Fracture. *Journal of the Mechanical Behaviour of Biomedical Materials*, Volume 126, p. 104957

Groen, B., Weerdesteyn, V., Duysens, J., 2008. The Relation between Hip Impact Velocity and Hip Impact Force Differs between Sideways Fall Techniques. *Journal of Electromyography and Kinesiology*, Volume 18(2), pp. 228–234

Kani, K., Porrino, J., Dahiya, M., Taljanovic, M., Mulcahy, H., Chew, F., 2016. A Visualization of the Greater Trochanter and Peritrochanteric Soft Tissues. *The American Academy of Physical Medicine and Rehabilitation*, Volume 9(3), pp. 318–324

Khakpour, S., Tanska, P., Esrafilian, A., Mononen, M.E., Saarakkala, S., Korhonen, R.K., Jämsä, T., 2021. Effect of Impact Velocity, Flooring Material, and Trochanteric Soft-Tissue Quality on Acetabular Fracture during a Sideways Fall: A Parametric Finite Element Approach. *Applied Sciences*, Volume 11(365), pp. 1–35

Kok, J., Grassi, L., Gustafsson, A., Isaksson, H., 2021. Femoral Strength and Strains in Sideways Fall: Validation of Finite Element Models Against Bilateral Strain Measurements. *Journal of Biomechanics*, Volume 122, p. 110445

Kroonenberg, V.D.A.J., Hayes, W.C., McMahon, T.A., 1995. Dynamic Models for Sideways Falls from Standing Height. *Journal of Biomedical Engineering*, Volume 117, pp. 309–318

Laing, A.C., Robinovitch, S.N., 2008. The Force Attenuation Provided by Hip Protectors Depends on Impact Velocity, Pelvic Size, and Soft Tissue Thickness. *Journal of Biomechanical Engineering*, Volume 130, pp. 1–9

Laing, A.C., Robinovitch, S.N., 2010. Characterizing the Effective Stiffness of the Pelvis During Sideways Falls on the Hip. *Journal of Biomechanics*, Volume 43, pp. 1898–1904

Laing, A.C., Tootoonchi, I., Hulme, P.A., Robinovitch, S.N., 2006. Effect of Compliant Flooring on Impact Force during Falls on the Hip. *Journal of Orthopaedic Research*, Volume 24(7), pp. 1405–1411

Li, N., Tsushima, E., Tsushima, H., 2013. Comparison of Impact Force Attenuation by Various Combinations of Hip Protector and Flooring Material using A Simplified Fall-Impact Simulation Device. *Journal of Biomechanics*, Volume 46, pp. 1140–1146

Lim, K.T., Choi. W.J., 2019. Soft Tissue Stiffness Over the Hip Increases with Age and Its Implication in Hip Fracture Risk in Older Adults. *Journal of Biomechanics*, Volume 93, pp. 28–33

Makhsous, M., Venkatasubraminian, G., Chawla, A., Pathak, Y., Priebe, M., Rymer, W.Z., Lin, F., 2008. Investigation of Soft-Tissue Stiffness Alteration in Denervated Human Tissue Using an Ultrasound Indentation System. *The Journal of Spinal Cord Medicine*, Volume 31(1), pp. 88–96

Nasiri, M., Luo, Y., 2016. Study of Sex Differences in the Association between Hip Fracture Risk and Body Parameters by DXA-Based Biomechanical Modeling. *Bone*, Volume 90, pp. 90–98

Nor-Izmin, N.A., Hazwani, F., Todo, M., Abdullah, A.H., 2020. Risk of Bone Fracture in Resurfacing Hip Arthroplasty at Varus and Valgus Implant Placements. *International Journal of Technology*, Volume 11(5), pp. 1025–1035

Radzevičienė, L., Ostrauskas, R., 2013. Body Mass Index, Waist Circumference, Waist-Hip Ratio, Waist-Height Ratio and Risk for Type 2 Diabetes in Women: A Case-Control Study. *Public Health*, Volume 127(3), pp. 241–246

Robinovitch, S.N., Hayes, W.C., McMahon, T.A., 1991. Prediction of Femoral Impact Forces in Falls on the Hip. *Journal of Biomechanical Engineering*, Volume 113, pp. 366–374

Robinovitch, S.N., Hayes, W.C., McMahon, T.A., 1995. Energy-Shunting Hip Padding System Attenuates Femoral Impact Force in a Simulated Fall. *Journal of Biomechanical Engineering*, Volume 117, pp. 409–413

Sarvi, M. N., Luo, Y., Sun, P., Ouyang J., 2014. Experimental Validation of Subject-Specific Dynamics Model for Predicting Impact Force in Sideways Fall. *Journal of Biomedical Science and Engineering*, Volume 07(07), pp. 405–418

Sarvi, M.N., Luo, Y., 2015. A Two-Level Subject-Specific Biomechanical Model for Improving Prediction of Hip Fracture Risk. *Clinical Biomechanics*, Volume 30(8), pp. 881–887

Sarvi, M.N., Luo, Y., 2017. Sideways Fall-Induced Impact Force and Its Effect on Hip Fracture Risk: A Review. *Osteoporosis International*, Volume 28(10), pp. 2759–2780

Sarvi, M.N., Luo. Y., 2019. Improving the Prediction of Sideways Fall-Induced Impact Force for Women by Developing a Female-Specific Equation. *Journal of Biomechanics*, Volume 88, pp. 64–71

Shaabpoor, E., Pavic, A., 2016. Human-structure Dynamic Interactions during Short-Distance Free Fall. *Shock and Vibration*, Volume 2016, pp. 1–12

Triwardono, K., Supriadi, S., Whulanza, Y., Saragih, A.S., Novalianita, D.A., Utomo, M.S., Kartika, I. 2021. Evaluation of the Contact Area in Total Knee Arthroplasty Designed for Deep Knee Flexion. *International Journal of Technology*, Volume 12(6), pp. 1312–1322

Zijden, V.D.A.M., Groen, B.E., Tanck, E., Nienhuis, B., Verdonschot, N., Weerdesteyn, V., 2017. Estimating Severity of Sideways Fall using a Generic Multi-Linear Regression Model Based on Kinematic Input Variables. *Journal of Biomechanics*, Volume 54, pp. 19–25